# Structural, morphological and electrical properties of (MgO) thin films doped with (ZnS) prepared by chemical spray pyrolysis method

**Hussein S. Al-Rikabi [1*], Muhammad Hameed AL-TIMIMI[2], Mustafa Zaid Abdullah[3], Widad H. ALBANDA[4]**

## Abstract

Thin films of magnesium oxide (MgO) doped with zinc sulfide (ZnS) were deposited on glass substrates at (350 °C) by the spray pyrolysis technique. The structural properties, surface morphology, and electrical properties of all the prepared films were studied. An X-ray diffraction study confirms the successful fabrication of pure (MgO) thin films and doped with (ZnS) sulfide. The surface morphology revealed by (FE-SEM) of the films reveals that the morphology of the (MgO) films changes dramatically with increasing (ZnS) doping concentration. Through Hall effect measurements, the type of charge carriers of the prepared films was identified and found to be (n-type) for pure (MgO) films and doped with (2 and 4%) of zinc sulfide (ZnS), while they converted to (p-type) for films doped with (6 and 8%) of zinc sulfide (ZnS).

**Key Words:** Thin films, MgO, ZnS, Hall effect, Spray pyrolysis technique.

**DOI Number: 10.14704/nq.2022.20.1.NQ22001** **NeuroQuantology 2022; 20(1):01-08**



## Introduction

Thin films of magnesium oxide (MgO) have an important scientific and technological role due to their practical properties (Carta et al., 2007a; Carta et al., 2007b). In addition, Magnesium Oxide (MgO) has a wide bandgap and remarkable chemical and thermal stability (Carta et al., 2007a; Moses Ezhil Raj, Nehru, Jayachandran, & Sanjeeviraja, 2007). Thin MgO films are used in solar cell applications, sensors, light-emitting diodes, and optoelectronic devices (Carta et al., 2007a; Moses Ezhil Raj et al., 2007; Visweswaran, Venkatachalapathy, Haris, & Murugesan, 2020). Doping is a useful technology that significantly modifies the properties of host materials. To modify the properties of thin films (MgO), many doping were used, including (Ag, Al, Cr, Fe, Zn) (Benedetti, Nilius, & Valeri, 2015; Islam, Rahman, Farhad, & Podder, 2019; Maiti et al., 2017; Nion et al., 2021; Yu, 2018). In this work, we chose zinc sulfide (ZnS) as the doping component because zinc sulfide (ZnS) is a low-toxicity, low-cost, and readily available substance (Goktas, Tumbul, Aba, Kilic, & Aslan, 2020). Moreover, (ZnS) is a composite (II-VI) semiconductor with a high refractive index and bandgap (3.72 eV at room temperature) and is used in many different technological applications (Ashokkumar & Boopathyraja, 2018). Thin (MgO) films can be deposited by various techniques, including electron beam evaporation (Saeed, Al-Timimi, & Hussein, 2021; Yu, 2018), (sol-gel) (Ho, Xu, & Mackenzie, 1997), spraying (Benedetti et al., 2015), chemical vapor deposition (CVD)

**Corresponding author:** Hussein S. Al-Rikabi
**Address:** 1* Department of Physics, College of Science, University of Diyala, Iraq.
Email: sciphyms2104@uodiyala.edu.iq

(Talukdar et al., 2018), spin coating (Güngör, USLU, Güngör, & BÖBREK, 2020), spray pyrolysis technology (Tlili, Jebbari, Naffouti, & Kamoun, 2020), etc. The spray pyrolysis technique, compared to the previous techniques, is simple in cost and can deposit films in a large area (Kabir et al., 2021; Kabir, Rahman, & Khan, 2018). In the current work, the structural, morphological surface, and electrical properties of the (MgO) films doped with (ZnS) were studied using the spray pyrolysis technique.



## Experimental details

Pure (MgO) thin films doped with zinc sulfide (ZnS) were prepared by spray pyrolysis on glass substrates at (350 °C). (0.1M) of magnesium chloride (MgCl2.6H2O) was used to get (MgO) and (0.1M) of zinc nitrate (Zn(NO3).6H2O) and thiourea (CH4N2S) to get (ZnS) all dissolved in distilled water . Thin (MgO) films and doped were obtained with different volumetric ratios (0, 2, 4, 6, 8) % of (ZnS) after spraying the solution with a compressor at (1.5 bar) on glass substrates. The structural properties were measured using X-ray diffraction (XRD), surface morphological by field emission scanning electron microscopy (FESEM), and electrical properties using Hall effect measurement for all the prepared films.

## Results and discussion

Fig. 1 shows the (XRD) patterns of pure magnesium oxide (MgO) and doped with different volumetric ratios (2, 4, 6, and 8 %) of zinc sulfide. The diagnostic peaks (Characteristic Peaks) showed that pure magnesium oxide (MgO) was obtained with a cubic crystal structure (F23 no.196) with crystalline dimensions (a=b = c = 4.22 Å) and angles (α=β=γ= 90°). As shown in Fig. 1a, which matches the Standard Pattern (JCPDS 01-074-1225). From Fig. 1, we notice that the process of doping with zinc sulfide (ZnS) led to a decrease in the intensity (Low Intensity) and an increase in the width of the diagnostic peaks with an increase in the percentage of doping, This is due to the substitution of (Mg) ions with sulfur and zinc ions (Zn+2 and S-2 ions), the diffusion of ions within the crystal lattice of magnesium oxide (MgO), and the emergence of new peaks after the doping process at the corners ( 2Θ= 28.7°, 47.56°, 56.38°) for the (0117) (110) (1148) crystalline levels, indicating the formation of a hexagonal (ZnS) Crystal Structure (P63mc no.163) with crystalline dimensions (a=b = 3.82 Å, c = 6.25 Å) () and angles (α=β=90°, γ=120°), which corresponds to standard spectrum (JCPDS 00-002-1310). The results showed that the crystalline growth of magnesium oxide (MgO) in the same cubic system after the doping process with zinc sulfide (ZnS) had no other peaks, indicating the presence of impurities within the prepared material. On the other hand, the results obtained showed that there is a very small (Negligible Shift) shift in the diagnostic peaks of magnesium oxide (MgO) towards the lowest angles after the doping process, which is due to the replacement and diffusion of sulfur ions and zinc ions (Zn+2, S-2) in the crystal lattice to magnesium oxide (MgO) and forms the zinc hexagonal sulfide phase [18, 19]. Crystalline size was calculated using the Debye-Scherrer equation for magnesium oxide (MgO) particles before and after doping with zinc sulfide (ZnS) as shown in Table 1. The results showed a slight decrease in the crystalline size of the prepared magnesium oxide nanoparticles (MgO) with an increase in the percentage of doping, which can be explained on the basis of the distribution of positive ions (Cations) as a result of replacing the magnesium ion (Mg+2) with ionic radius the smallest (Mg+2 = 0.66 Å) with zinc ions (Zn+2) has the largest ionic radius (0.74 Å) which leads to an increase in intrinsic stress and an increase in the values of micro strain. Thus, the crystallite qualities deteriorate and thus the crystal size decreases [18-21].

**Table 1.** Shows The Crystalline Size Values and Some Crystalline Parameters for the prepared thin films.

| Sample | 2Θ (deg) Practical | 2Θ (deg) Standard | FWHM (deg) | Crystalline size (nm) | dhkl (Å) Practical | dhkl (Å) Standard | (hkl) |
|---|---|---|---|---|---|---|---|
| MgO | 42.82 | 42.82 | 0.3694 | 20.02 | 2.110 | 2.11 | (200) |
| MgO 0.98ZnS0.02 | 42.72 | 42.82 | 0.5713 | 12.95 | 2.114 | 2.11 | (200) |
| MgO 0.96 ZnS0.04 | 42.69 | 42.82 | 0.5627 | 13.14 | 2.116 | 2.11 | (200) |
| MgO 0.94 ZnS0.06 | 42.65 | 42.82 | 0.7068 | 10.47 | 2.118 | 2.11 | (200) |
| MgO 0.92 ZnS0.08 | 42.65 | 42.82 | 0.9472 | 7.81 | 2.114 | 2.11 | (200) |

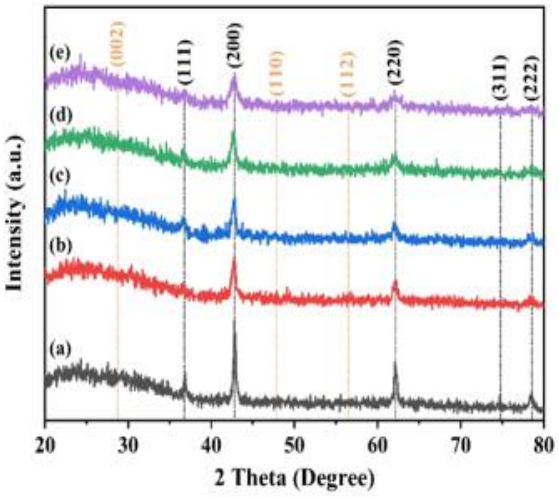

**Figure 1.** X-ray diffraction patterns of thin films (MgO) doped with zinc sulfide (ZnS): (a) (MgO) pure, (b) 2% (ZnS), (c) 4% (ZnS), (d) 6% (ZnS), (e) 8% (ZnS)

## Surface morphology

The morphology of the surfaces of all the prepared films was studied using field emission scanning electron microscopy (FE-SEM), which provides us with images of the surfaces with high resolution and magnification. Fig. 2, 3, 4, 5, and 6 Illustrate the (FE-SEM) images with the grain size distribution scheme for all the prepared films. We note that the prepared films' surface structures consist of aggregates of dense quasi-spherical nanoparticles and highly agglomerated. This is consistent with (Abdul-Hamead, 2020; Suresh, 2014), and the rate of grain size decreases with an increasing percentage of doping with zinc sulfide (ZnS), and this agrees with the researcher (Rajendran, Deepa, & Mekala, 2018). which confirms the spread of sulfur and zinc ions within the crystal lattice of magnesium oxide (MgO) (Lad, Kokode, Deore, & Tupe). The largest value for the average grain size was for the pure (MgO) film, while the lowest value was for the doped film by (8%) of zinc sulfide (ZnS).

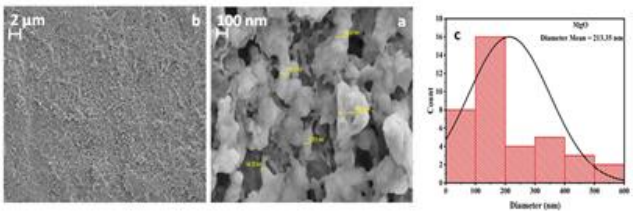


**Figure 2.** (a,b) (FE-SEM) images, (c) grain size distribution diagram of the thin film (MgO).

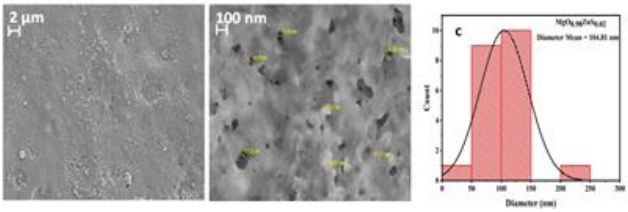


**Figure 3.** (a,b) (FE-SEM) images, (c) grain size distribution diagram of the thin film ($MgO_{0.98}ZnS_{0.02}$).

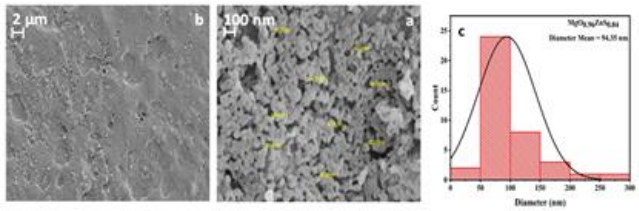


**Figure 4.** (a,b) (FE-SEM) images, (c) grain size distribution diagram of the thin film ($MgO_{0.96}ZnS_{0.04}$).

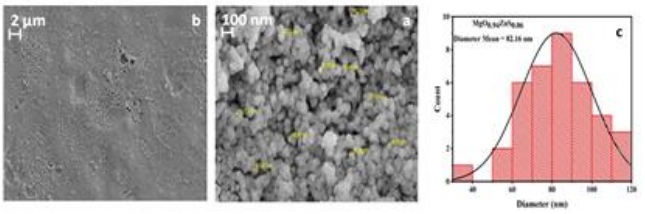


**Figure 5.** (a,b) (FE-SEM) images, (c) grain size distribution diagram of the thin film ($MgO_{0.94}ZnS_{0.06}$).

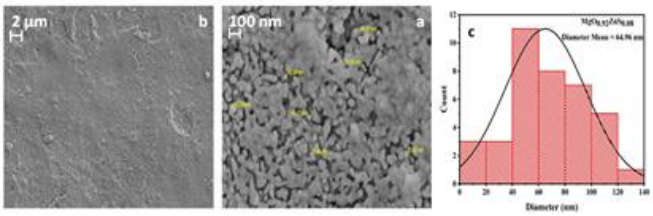


**Figure 6.** (a,b) (FE-SEM) images, (c) grain size distribution diagram of the thin film ($MgO_{0.92}ZnS_{0.08}$).

## Electrical Measurement



The Hall effect measurements were studied for (MgO) thin films doped with zinc sulfide (ZnS) with different volumetric ratios (0, 2, 4, 6, and 8%). It was found that the type of charge carriers of the films of pure magnesium oxide (MgO) and doped with (2%, 4%) of zinc sulfide (ZnS) are of the negative type (n-type) from the value of the negative Hall coefficient (RH), and this agrees with researcher (Wan et al., 2017), While the type of charge carriers for (MgO) films doped with (6%, 8%) of zinc sulfide (ZnS) is of the positive type (p-type) from the value of the positive Hall factor (RH) due to the high percentage of positive charge carriers relative to carriers with the negative charge generated from the presence of zinc sulfide (ZnS) metal, and this agrees with the researcher (Mares, Boutwell, Scheurer, Falanga, & Schoenfeld, 2010), Table 2. Shows the results of the Hall effect measurements, as we notice an increase in the values of Hall's coefficient by increasing the percentage of doping with zinc sulfide (ZnS) until it reaches its highest value at the membrane (MgO0.94ZnS0.06). The results showed that the values of the resistivity for all films were high, and the highest value was for the films doped with (4%) of zinc sulfide (ZnS). While the conductivity values were low for all the prepared films, they also increased after doping with zinc sulfide (ZnS), and their highest value was for the film doped with (8%) of zinc sulfide (ZnS). The high values of resistivity are caused by defects in the crystal structure of the film that restrict the movement of charge carriers (Manjula, Balu, Usharani, Raja, & Nagarethinam, 2016), As for mobility, its values decreased with the increase in the percentage of doping with zinc sulfide (ZnS), and the lowest value

was for the film doped with (6%) of zinc sulfide (ZnS). Fig. 7 Shows the values of each of the resistivity, Hall's modulus, and the concentration of charge carriers as a function of doping ratios for all the prepared films.

**Table 2.** Hall effect measurements for the prepared thin films.

| Sample | Concentration $(cm)^{-3}$ | Hall Coefficient $R_H$ $(m^2/C)$ | Conductivity $(\Omega.cm)^{-1}$ | Resistivity $(\Omega.cm)$ | Mobility $(cm^2/v.s)$ |
|---|---|---|---|---|---|
| MgO | $-19.31\times10^{11}$ | $-0.3233\times10^{7}$ | $0.2144\times10^{-6}$ | $4.663\times10^{6}$ | $0.6932\times10^{2}$ |
| $MgO_{0.98}ZnS_{0.02}$ | $-3.069\times10^{11}$ | $-2.0340\times10^{7}$ | $3.3690\times10^{-6}$ | $0.2968\times10^{6}$ | $0.6852\times10^{2}$ |
| $MgO_{0.96}ZnS_{0.04}$ | $-1.231\times10^{11}$ | $-5.071\times10^{7}$ | $1.001\times10^{-6}$ | $9.987\times10^{6}$ | $0.5078\times10^{2}$ |
| $MgO_{0.94}ZnS_{0.06}$ | $0.5887\times10^{11}$ | $10.60\times10^{7}$ | $0.3973\times10^{-6}$ | $2.517\times10^{6}$ | $0.4213\times10^{2}$ |
| $MgO_{0.92}ZnS_{0.08}$ | $2.675\times10^{11}$ | $2.333\times10^{7}$ | $7.0160\times10^{-6}$ | $0.1425\times10^{6}$ | $1.637\times10^{2}$ |

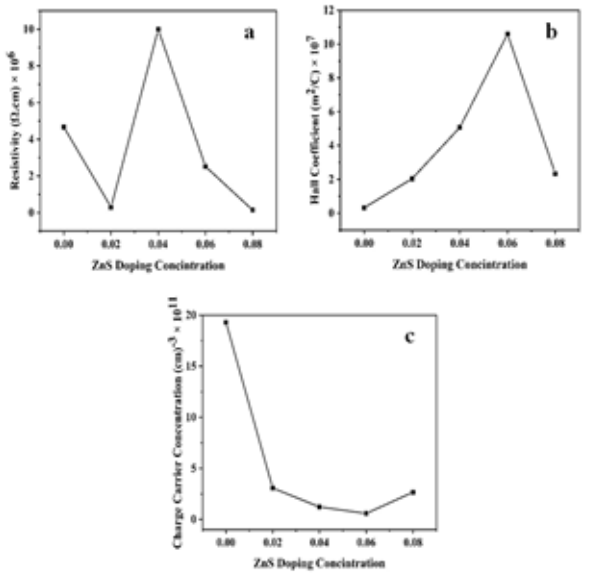


**Figure 7.** shows the values of (a) resistivity, (b) Hall coefficient, and (c) concentration of charge carriers, as a function of doping ratios for all prepared films.

## Conclusion

The results of X-ray diffraction (XRD) assays showed that the thin films of pure magnesium oxide (MgO) doped with zinc sulfide (ZnS) have a polycrystalline structure with a favorable direction of growth (200). The results of the scanning field emitting electron microscope (FE-SEM) assays showed that the prepared films have a nanostructure and their surface consists of dense semi-spherical grains, and that the grain size average values decrease with an increasing percentage of doping with zinc sulfide (ZnS). The results of the Hall effect measurements showed that the charge carriers of pure (MgO) thin films and those doped with (2%, 4%) zinc sulfide (ZnS) of (n-type) and the films doped with (6%, 8%) of zinc sulfide (ZnS) became p-type charge carriers. Through the results of the structural and electrical tests, it was found that the (MgO) films can control their properties by doping with zinc sulfide (ZnS), and the prepared films can be used in solar cell applications.

## References

Abdul-Hamead, A. A. (2020). Advanced Structured of MgO Thin Film for Bio Applications. Paper presented at the Materials Science Forum.

Ashokkumar, M., & Boopathyraja, A. (2018). Structural and optical properties of Mg doped ZnS quantum dots and biological applications. Superlattices and Microstructures, 113, 236-243.

Benedetti, S., Nilius, N., & Valeri, S. (2015). Chromium-doped MgO thin films: morphology, electronic structure, and segregation effects. The Journal of Physical Chemistry C, 119(45), 25469-25475.

Carta, G., El Habra, N., Crociani, L., Rossetto, G., Zanella, P., Zanella, A., . . . Tondello, E. (2007a). CVD of MgO thin films from bis (methylcyclopentadienyl) magnesium. Chemical vapor deposition, 13(4), 185-189.

Carta, G., El Habra, N., Crociani, L., Rossetto, G., Zanella, P., Zanella, A., . . . Tondello, E. J. C. v. d. (2007b). CVD of MgO thin films from bis (methylcyclopentadienyl) magnesium. 13(4), 185-189.

Goktas, A., Tumbul, A., Aba, Z., Kilic, A., & Aslan, F. (2020). Enhancing crystalline/optical quality, and photoluminescence properties of the Na and Sn substituted ZnS thin films for optoelectronic and solar cell applications; a comparative study. Optical Materials, 107, 110073.

Güngör, T., USLU, B., Güngör, E., & BÖBREK, A. (2020). Arduino Based Thin Film Spin Coating System Design and MgO Thin Film Preparation.

Ho, I.-C., Xu, Y., & Mackenzie, J. D. (1997). Electrical and optical properties of MgO thin film prepared by sol-gel technique. Journal of Sol-Gel Science and Technology, 9(3), 295-301.

Islam, M. R., Rahman, M., Farhad, S., & Podder, J. (2019). Structural, optical and photocatalysis properties of sol–gel deposited Al-doped ZnO thin films. Surfaces and Interfaces, 16, 120-126.

Kabir, M. H., Bhattacharjee, A., Islam, M. M., Rahman, M., Rahman, M., & Khan, M. (2021). Effect of Sr doping on structural, morphological, optical and electrical properties of spray pyrolized CdO thin films. Journal of Materials Science: Materials in Electronics, 32(3), 3834-3842.

Kabir, M. H., Rahman, M., & Khan, M. (2018). Influence of Al doping on microstructure, morphology, optical and photoluminescence properties of pyrolytic ZnO thin films prepared in an ambient atmosphere. Chinese Journal of Physics, 56(5), 2275-2284.

Lad, U. D., Kokode, N., Deore, M. B., & Tupe, U. J. MgO INCORPORATED ZnO NANOSTRUCTURED BINARY OXIDE THIN FILM ETHANOL GAS SENSOR.

Maiti, P., Das, P. S., Bhattacharya, M., Mukherjee, S., Saha, B., Mullick, A. K., & Mukhopadhyay, A. K. (2017). Transparent Al+ 3 doped MgO thin films for functional applications. Materials Research Express, 4(8), 086405.

Manjula, N., Balu, A., Usharani, K., Raja, N., & Nagarethinam, V. (2016). Enhancement in some physical properties of spray deposited CdO: Mn thin films through Zn doping towards optoelectronic applications. Optik, 127(16), 6400-6406.

Mares, J., Boutwell, C., Scheurer, A., Falanga, M., & Schoenfeld, W. (2010). Cubic ZnxMg1-xO and NixMg1-xO thin films grown by molecular beam epitaxy for deep-UV optoelectronic applications. Paper presented at the Oxide-based Materials and Devices.

Moses Ezhil Raj, A., Nehru, L., Jayachandran, M., & Sanjeeviraja, C. (2007). Spray pyrolysis deposition and characterization of highly (100) oriented magnesium oxide thin films. Crystal Research and Technology: Journal of Experimental and Industrial Crystallography, 42(9), 867-875.

Nion, M. G. M., Kabir, M. H., Mona, M. A., Haque, M. J., Shahariar, N., Hafiz, M., & Rahman, M. (2021). Effect of Al doping on morphology and optical properties of spray pyrolized MgO thin films. Results in Materials, 12, 100235.

Rajendran, V., Deepa, B., & Mekala, R. (2018). Studies on structural, morphological, optical and antibacterial activity of Pure and Cu-doped MgO nanoparticles synthesized by co-precipitation method. Materials Today: Proceedings, 5(2), 8796-8803.

Saeed, M., Al-Timimi, M., & Hussein, O. (2021). Structural, morphological and optical characterization of nanocrystalline WO3 thin films. DIGEST JOURNAL OF NANOMATERIALS AND BIOSTRUCTURES, 16(2), 563-569.

Suresh, S. (2014). Investigations on synthesis, structural and electrical properties of MgO nanoparticles by sol–gel method. Ovonic Res, 10, 205.

Talukdar, T. K., Liu, S., Zhang, Z., Harwath, F., Girolami, G. S., & Abelson, J. R. (2018). Conformal MgO film grown at high rate at low temperature by forward-directed chemical vapor deposition. Journal of Vacuum Science & Technology A: Vacuum, Surfaces, and Films, 36(5), 051504.

Tlili, M., Jebbari, N., Naffouti, W., & Kamoun, N. T. (2020). Effect of precursor nature on physical properties of chemically sprayed MgO thin films for optoelectronic application. The European Physical Journal Plus, 135(8), 1-12.

Visweswaran, S., Venkatachalapathy, R., Haris, M., & Murugesan, R. (2020). Characterization of MgO thin film prepared by spray pyrolysis technique using perfume atomizer. Journal of Materials Science: Materials in Electronics, 31(17), 14838-14850.

Wan, Y., Samundsett, C., Bullock, J., Hettick, M., Allen, T., Yan, D., . . . Javey, A. (2017). Conductive and stable magnesium oxide electron-selective contacts for efficient silicon solar cells. Advanced Energy Materials, 7(5), 1601863.

Yu, H. K. (2018). Secondary electron emission properties of Zn-doped MgO thin films grown via electron-beam evaporation. Thin Solid Films, 653, 57-61.